EPJ Web of Conferences **198**, 00002 (2019) https://doi.org/10.1051/epjconf/201919800002
QTech 2018

Quantum temporal imaging with squeezed light

Giuseppe Patera[1,*], *Dmitri* Horoshko[1,2], and *Mikhail* Kolobov[1]

[1]Univ. Lille, CNRS, UMR 8523 - PhLAM - Physique des Lasers Atomes et Molécules, F-59000 Lille, France

[2]B. I. Stepanov Institute of Physics, NASB, Nezavisimosti Ave. 68, Minsk 220072 Belarus

Abstract. We consider a simple quantum temporal imaging system on the basis of a time lens implemented by a parametric nonlinear optical process with a chirped pump. We review the main results of the modal theory of temporal imaging, developed recently by us. We illustrate this theory by a concrete example of type-I non-collinear sum-frequency generation process, where the phase matching is limited by the temporal walk-off of the signal and the idler waves. We have shown that the temporal modal functions of such an imaging system are chirped Hermite-Gauss functions.

1 Introduction

Quantum temporal imaging is a technique for the manipulation of the time-frequency degrees of freedom of a quantum state and it is based on the space-time duality of optical processes [1, 2]. By virtue of this duality a device able to imprint onto an incoming wavefront a quadratic phase modulation in time is called time-lens. Time-lenses possessing enough bandwidth for manipulating ultrafast pulses are based on non-linear processes such as three- [3–5] or four-wave mixing [6, 7]. In quantum communication and networking, optical processing of information may be accompanied by quantum noise, negligible in classical regime, but detrimental for fragile quantum states of light. Strategies for manipulation of single-photon fields by temporal imaging technique have been considered for quantum optical pulse shaping [8], bandwidth compression [9], temporal imaging of time-bin entangled photonic wave packets [10], and manipulation of single-photon waveforms [11]. These results are especially important in the light of recent advances in generation of ultrabroadband biphotons by means of chirped quasi-phase-matched crystals [12, 13]. This technology allows one to transmit quantum information at rates of tens and hundreds of THz, however its decoding requires significant temporal stretching to fit the single-photon detector bandwidth, which is of the order of 10 GHz.

Recently the theory of quantum temporal imaging has been applied to squeezed light [14–16]. The techniques of sum-frequency generation [14] and four-wave mixing [15] with perfect phase-matching have been considered. The limits of validity for perfect phase-matching approximation and the quantum field of view have been studied [16]. These results are important for optical implementations of quantum information protocols with continuous variables.

*e-mail: Giuseppe.Patera@univ-lille.fr

In particular, quantum temporal stretching provides a method of decoding quantum information, conveyed by ultrabroadband squeezed light, which is generated in chirped quasi-phase-matched crystals [17–19]. Application of temporal imaging technique to continuous quantum variables requires a close to 100% efficiency of the frequency conversion process [10, 14–16].

Quantum temporal imaging of continuous variables has been considered in the limit of infinite temporal aperture and perfect phase-matching [14, 15], in the limit of finite aperture but still perfect phase-matching [20, 21], and recently, for the imperfect phase-matching [22], where the eigenmodes of the imaging system were found in the frequency domain. In the present work we develop the latter approach and study the eigenmodes of the quantum temporal system in the temporal domain.

2 Quantum field transformation in a temporal imaging system

We consider the simplest imaging scheme that can be realized with a single time lens. It consists in first (*input*) dispersive medium followed by a time lens then followed by a second (*output*) dispersive medium [22]. The time lens is implemented by a sum frequency generation (SFG) process with the signal and the pump waves having the same frequency and polarization [3–5, 16]. A pulse at signal carrier frequency ω_s after a dispersive propagation through the input medium is up-converted by SFG to a new pulse at the idler carrier frequency $\omega_\mathrm{i} = \omega_\mathrm{i} - \omega_\mathrm{s}$. Finally the idler pulse is dispersed through the output medium.

All interacting field are accepted to be plane waves, propagating along the z axis, and each field is described by its positive-frequency part $\hat{E}_m^{(+)}(t,z)$, where the index $m = \{\mathrm{s},\mathrm{i},\mathrm{p}\}$ identifies the signal, idler or pump waves respectively. For each wave we define the envelope $\hat{A}_m(t,z)$ by separating the fast optical oscillations on the carrier frequency ω_m with the corresponding wave vector $k_m = k(\omega_m)$:

$$\hat{E}_m^{(+)}(t,z) = \mathcal{E}_m \, \mathrm{e}^{\mathrm{i}(k_m z - \omega_m t)} \hat{A}_m(t,z), \tag{1}$$

where $\mathcal{E}_m$ is the one-photon amplitude, scaling the envelope function to the photonic units.

It is convenient to define a travelling-wave frame of reference (τ,ξ) propagating at pulse group velocity such that $\xi = z$, $\tau = t - k'z$, with $k' = (\mathrm{d}k/\mathrm{d}\Omega)_{\Omega=0}$ for the corresponding wave. In this frame of reference we have

$$\hat{A}_m(\tau,\xi) = \int \frac{\mathrm{d}\Omega}{2\pi} \, \mathrm{e}^{\mathrm{i}\,\delta_m(\Omega)\xi - \mathrm{i}\Omega\tau} \hat{a}_m(\Omega,\xi), \tag{2}$$

where $\delta_m(\Omega) = k(\omega_m + \Omega) - k_m - \beta_1\Omega$.

In order that the SFG interaction realizes a time lens, the pump should have a quadratic in time phase dependence. For a Gaussian pump pulse such a dependence can be rather easily realized by impinging a quadratic frequency phase shift by propagation in a dispersive medium with the total group delay dispersion (GDD) $-D_\mathrm{f}$. Thus, the classical pump wave in the SFG crystal is described by its amplitude

$$\alpha_\mathrm{p}(\Omega) = A_\mathrm{p} \mathrm{e}^{-\frac{1}{2}\Omega^2/\Delta_\mathrm{p}^2 + \frac{\mathrm{i}}{2} D_\mathrm{f}\Omega^2}, \tag{3}$$

which does not depend on ξ because the pump is accepted to be undepleted and its broadening by the SFG medium is neglected. The spectral width of the pump pulse Δ_p is related to the full width at half maximum (FWHM) of its temporal intensity profile τ_p as $\Delta_\mathrm{p} = 2\sqrt{\ln 2}\tau_\mathrm{p}^{-1}$.

In the considered case of SFG the pump and the signal waves travel at the same group velocities, while the idler wave, having a higher carrier frequency, is delayed by the temporal walk-off time $\tau_i = |k'_p - k'_i|L$ [16], where L is the length of the SFG crystal. Gaussian modelling

of the phase-matching function is possible if $\mathrm{sinc}(x)$ is replaced by $\mathrm{e}^{-x^2/(2\sigma_0^2)}$, where $\sigma_0 = 1.61$ is chosen so that these two functions have the same width at half-maximum [23]. Then the phase-matching function [16] can be approximated as $\mathrm{sinc}(\tau_i\Omega/2) \approx \mathrm{e}^{-\frac{1}{2}\Omega^2/\Delta_v^2}$, where the characteristic phase-matching bandwidth in the idler frequency is $\Delta_v = 2\sigma_0\tau_i^{-1}$.

Under these conditions the output field of the quantum temporal imaging system can be written [20, 22]

$$\hat{a}_{\mathrm{i}}^{\mathrm{out}}(\Omega) = \int \mathrm{d}\Omega' \left[\mu(\Omega,\Omega')\hat{a}_{\mathrm{s}}^{\mathrm{in}}(\Omega') + \nu(\Omega,\Omega')\hat{a}_{\mathrm{i}}^{\mathrm{in}}(\Omega')\right], \tag{4}$$

where $\mu(\Omega,\Omega')$ and $\nu(\Omega,\Omega')$ are two transfer functions in frequency satisfying the relation

$$\int \mathrm{d}\Omega'' \left[\mu(\Omega,\Omega'')\mu^*(\Omega',\Omega'') + \nu(\Omega,\Omega'')\nu^*(\Omega',\Omega'')\right] = \delta(\Omega-\Omega'), \tag{5}$$

required by the unitarity of Eq. (4). The transfer functions can be represented in the form of their singular value decompositions

$$\mu(\Omega,\Omega') = \sum_{m=0}^{\infty} \sin(\lambda_m)\psi_m(\Omega)\varphi_m^*(\Omega'), \tag{6}$$

$$\nu(\Omega,\Omega') = \sum_{m=0}^{\infty} \cos(\lambda_m)\psi_m(\Omega)\zeta_m^*(\Omega'), \tag{7}$$

where the singular values are determined by the relation

$$\lambda_m = gA_{\mathrm{p}}L\left[\frac{2\pi\Delta_p\Delta_v}{F+1}\left(\frac{F-1}{F+1}\right)^m\right]^{1/2}, \tag{8}$$

with g being the wave coupling constant in the SFG crystal and $F = \sqrt{1+D_{\mathrm{f}}^2\Delta_p^2\Delta_v^2}$. The eigenfunctions are defined as follows

$$\psi_m(\Omega) = h_m\left(\frac{\sqrt{F}\Omega}{\Delta_v}\right)\left(\frac{\sqrt{F}}{\Delta_v}\right)^{1/2} \mathrm{e}^{\frac{\mathrm{i}}{2}D_{\mathrm{f}}(1+|M|)\Omega^2}, \tag{9}$$

$$\varphi_m(\Omega) = h_m\left(\frac{\sqrt{F}\Omega}{\Delta_p}\right)\left(\frac{\sqrt{F}}{\Delta_p}\right)^{1/2} \mathrm{e}^{\frac{\mathrm{i}}{2}D_{\mathrm{f}}(1/|M|+\Delta_v^2/\Delta_{\mathrm{p}}^2)\Omega^2}, \tag{10}$$

$$\zeta_m(\Omega) = h_m\left(\frac{\sqrt{F}\Omega}{\Delta_v}\right)\left(\frac{\sqrt{F}}{\Delta_v}\right)^{1/2}, \tag{11}$$

where $h_m(x)$ is the Hermite-Gauss function and M is the magnification of the temporal imaging system. The functions Eqs. (9)-(11) define frequency modes of the input and output fields of the imaging system. In the next section we consider the corresponding temporal modes.

3 Temporal eigenmodes of the temporal imaging system

In this section we consider a concrete example of temporal imaging system, close to that realized in Ref. [24]. The time lens in this experiment was realised by a 500 μm thick beta-barium borate (BBO) crystal cut at 28.1° and used in a non-collinear type-I phase-matching configuration with the pump and the signal centered at 830 nm and the idler centered at 415 nm. The temporal walk-off time for the signal and the idler waves in this configuration was

about $\tau_i = 100$ fs. We consider a pump pulse width of 3 fs and the focal GDD of the time lens 60 fs^2, which is much less than the corresponding values of Ref. [24]. This regime corresponds to $F = 1.48$ and to the characteristic input time $\tau_{\rm in} = \sqrt{F}/\Delta_p = 2.2$ fs. We put the magnification of the temporal imaging system to $|M| = 3$. In this case the modal functions of the two first input modes read

$$\varphi_0(\Omega) = \pi^{-1/4}\sqrt{\tau_{\rm in}}\mathrm{e}^{-\frac{1}{2}(1-id_{\rm in})(\tau_{\rm in}\Omega)^2}, \tag{12}$$

$$\varphi_1(\Omega) = \pi^{-1/4}\sqrt{2\tau_{\rm in}}\tau_{\rm in}\Omega\mathrm{e}^{-\frac{1}{2}(1-id_{\rm in})(\tau_{\rm in}\Omega)^2}, \tag{13}$$

where we have introduced the dimensionless input chirp $d_{\rm in} = D_{\rm f}(1/|M| + \Delta_v^2/\Delta_{\rm p}^2)\tau_{\rm in}^{-2} \approx 4.13$. We see that the family of input modes is completely determined by two parameters $\tau_{\rm in}$ and $d_{\rm in}$. The temporal modes can be found by the inverse Fourier transform, giving

$$\Phi_0(\tau) = \frac{\pi^{-1/4}}{\sqrt{2\pi\tau_{\rm in}}}\frac{1}{\sqrt{1-id_{\rm in}}}\mathrm{e}^{-\frac{1}{2\left(1+d_{\rm in}^2\right)}(\tau/\tau_{\rm in})^2(1+id_{\rm in})-i\omega_s\tau}, \tag{14}$$

$$\Phi_1(\tau) = \frac{\pi^{-1/4}}{\sqrt{\pi\tau_{\rm in}}}\frac{-i}{\sqrt{(1-id_{\rm in})^3}}\frac{\tau}{\tau_{\rm in}}\mathrm{e}^{-\frac{1}{2\left(1+d_{\rm in}^2\right)}(\tau/\tau_{\rm in})^2(1+id_{\rm in})-i\omega_s\tau} \tag{15}$$

where we have also added the oscillations at the optical carrier frequency ω_s. These modal functions are shown in Fig. 1.

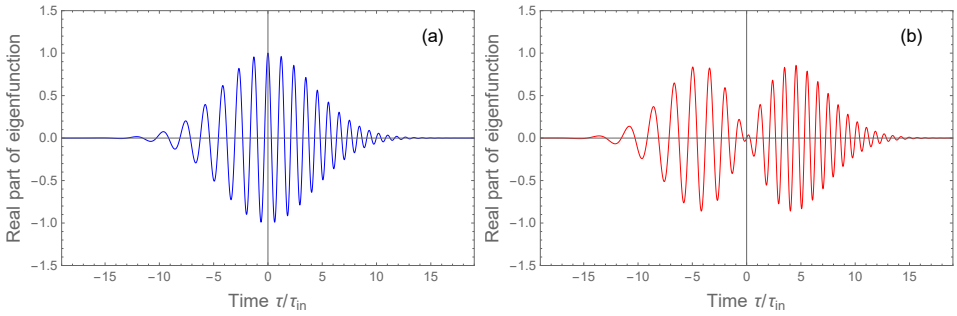

Figure 1. Input modal functions of the temporal imaging system: (a) $\Phi_0(\tau)$ and (b) $\Phi_1(\tau)$. Each function is a Hermite-Gauss function of the corresponding order with an additional chirp.

The output eigenfunctions have a different characteristic time $\tau_{\rm out} = \sqrt{F}/\Delta_v = 38$ fs and a different chirp parameter $d_{\rm out} = D_{\rm f}(1 + |M|)\tau_{\rm out}^{-2} \approx 0.17$. Their shapes can be obtained from Eqs. (14),(15) with the replacements $\tau_{\rm in} \to \tau_{\rm out}$ and $d_{\rm in} \to d_{\rm out}$. The fact that $d_{\rm in} \neq d_{\rm out}$ means that the output modes are different from the input ones even for the properly scaled time. The equality $d_{\rm in} = d_{\rm out}$ requires

$$|M| = \frac{\Delta_{\rm p}}{\Delta_v}, \tag{16}$$

implying $\tau_{\rm out} = |M|\tau_{\rm in}$, in which case the output modes are scaled $|M|$ times input modes, i.e. each mode is imaged independently of others [22]. This regime may be important for temporal imaging of multimode squeezed fields, where mixing the variables of different modes should be avoided.

4 Conclusions

In this work we considered quantum temporal imaging on the basis of a time lens implemented by a sum frequency generation process with a chirped pulse pump. We reviewed

the main results of the modal theory of temporal imaging and illustrated it by a concrete example. We have shown that the temporal modal functions of the imaging system eigenmodes are chirped Hermite-Gauss functions. These results may find numerous applications in experiments dealing with manipulation and detection of temporally multimode squeezed light.

Acknowledgments

This work was supported by the European Union's Horizon 2020 research and innovation programme under grant agreement No 665148 (QCUMbER).

References

[1] S.A. Akhmanov, A.P. Sukhorukov, A.S. Chirkin, J. Exp. Theor. Phys. **28**, 748 (1969)
[2] B.H. Kolner, IEEE J. Quantum Elect. **30**, 1951 (1994)
[3] C.V. Bennett, B.H. Kolner, IEEE J. Quantum Elect. **36**, 430 (2000)
[4] C.V. Bennett, B.H. Kolner, IEEE J. Quantum Elect. **36**, 649 (2000)
[5] V.J. Hernandez, C.V. Bennett, B.D. Moran, A.D. Drobshoff, D. Chang, C. Langrock, M.M. Fejer, M. Ibsen, Opt. Express **21**, 196 (2013)
[6] M.A. Foster, R. Salem, D.F. Geraghty, A.C. Turner-Foster, M. Lipson, A.L. Gaeta, Nature **456**, 81 (2008)
[7] O. Kuzucu, Y. Okawachi, R. Salem, M.A. Foster, A.C. Turner-Foster, M. Lipson, A.L. Gaeta, Opt. Express **17**, 20605 (2009)
[8] D. Kielpinski, J.F. Corney, H.M. Wiseman, Phys. Rev. Lett. **106**, 130501 (2011)
[9] M. Karpiński, M. Jachura, L.J. Wright, B.J. Smith, Nat. Photonics **11**, 53 (2017)
[10] Y. Zhu, J. Kim, D.J. Gauthier, Phys. Rev. A **87**, 043808 (2013)
[11] J.M. Donohue, M.D. Mazurek, K.J. Resch, Phys. Rev. A **91**, 033809 (2015)
[12] S. Sensarn, G.Y. Yin, S.E. Harris, Phys. Rev. Lett. **104**, 253602 (2010)
[13] M.B. Nasr, S. Carrasco, B.E.A. Saleh, A.V. Sergienko, M.C. Teich, J.P. Torres, L. Torner, D.S. Hum, M.M. Fejer, Phys. Rev. Lett. **100**, 183601 (2008)
[14] G. Patera, M.I. Kolobov, Opt. Lett. **40**, 1125 (2015)
[15] J. Shi, G. Patera, M.I. Kolobov, S. Han, Opt. Lett. **42**, 3121 (2017)
[16] G. Patera, J. Shi, D.B. Horoshko, M.I. Kolobov, J. Opt. **19**, 054001 (2017)
[17] D.B. Horoshko, M.I. Kolobov, Phys. Rev. A **88**, 033806 (2013)
[18] D.B. Horoshko, M.I. Kolobov, Phys. Rev. A **95**, 033837 (2017)
[19] M.V. Chekhova, S. Germanskiy, D.B. Horoshko, G.K. Kitaeva, M.I. Kolobov, G. Leuchs, C.R. Phillips, P.A. Prudkovskii, Opt. Lett. **43**, 375 (2018)
[20] G. Patera, D. Horoshko, M. Kolobov, arXiv:1806.11181
[21] J. Shi, G. Patera, Y. Gui, M.I. Kolobov, D.B. Horoshko, S. Han, Chin. Opt. Lett. **16**, 092701 (2018)
[22] G. Patera, D.B. Horoshko, M.I. Kolobov, Proc. SPIE **10771**, 10771 (2018)
[23] W.P. Grice, A.B. U'Ren, I.A. Walmsley, Phys. Rev. A **64**, 063815 (2001)
[24] C.V. Bennett, B.H. Kolner, IEEE J. Quantum Elect. **37**, 20 (2001)